Interfacial charge transfer excitation with large optical nonlinearity in manganite heterostructure

doi: 10.1103/PhysRevB.72.224403

Interfacial charge transfer excitation with large optical nonlinearity in manganite heterostructure

Takuya Satoh,[1] Kenjiro Miyano,[1] Yasushi Ogimoto,[1,2] Hiroharu Tamaru,[1,3] and Sumio Ishihara[4]
[1]*Research Center for Advanced Science and Technology, The University of Tokyo, Tokyo 153-8904, Japan*
[2]*Devices Technology Research Laboratories, SHARP Corporation, 2613-1 Tenri, Nara 632-8567, Japan*
[3]*PRESTO, Japan Science and Technology Agency, 4-1-8 Honcho Kawaguchi, Saitama 332-0012, Japan*
[4]*Department of Physics, Tohoku University, Sendai 980-8578, Japan*
(Received 20 July 2005; published 5 December 2005)

Interfacial electronic states between $LaMnO_3$ and $SrMnO_3$ have been studied by second-harmonic (SH) spectroscopy. The SH contributions from bulk, surface, and interface were separated by measuring four distinct types of manganite thin films. In the SH spectra, we found a broad peak at 2 eV unique to the $LaMnO_3/SrMnO_3$ interface, which was assigned to interfacial charge transfer excitation based on a Hartree-Fock calculation. No metallic phase showed up at the interface. Experimental and theoretical second-order susceptibilities $\chi^{(2)}$ at the interface were estimated to be $\sim 10^{-6}$ esu, which is ten times as large as the highest $\chi^{(2)}$ value of $BaTiO_3$.

DOI: 10.1103/PhysRevB.72.224403 PACS number(s): 75.47.Lx, 73.20.−r, 42.65.Ky, 78.20.−e

The interface between two dissimilar materials has been of fundamental importance in basic research and applications. For example, manipulation of electrons in a field-effect transistor is the basis for modern day electronics and provides an arena for the study of two-dimensional electronic states. In addition to these well characterized systems, much attention has recently been paid to the interfaces that involve strongly correlated electron systems, in which one may hope that the strong correlation leads to a novel electronic state bound to the interface.[1] In this context, manganites are quite attractive since their electronic state is particularly sensitive to carrier doping, lattice constant, and external stimuli because of a subtle balance of spin, charge, orbital, and lattice degrees of freedom.[2] For example, photoinduced antiferromagnetic-ferromagnetic and insulator-metal transitions have been reported.[3,4] Due to the sensitivity, it is natural to expect that the electronic state at the interface between two different bulk manganites can be substantially different from the electronic states of the bulk phases. Appearance of unique phases, spin canting, and spin frustration have been suggested, which are driven by charge transfer, exchange interaction, and strain effect at the interface.[5,6] Making use of the half-metallic behavior of $La_{1-x}Sr_xMnO_3$, a tunneling magnetoresistance (TMR) device has been fabricated. The importance of the dead layer at the interface that prevents the TMR near the Curie temperature has been well demonstrated.[7]

The characterization of the interfaces is not straightforward, however, because many surface sensitive approaches, e.g., scanning probe microscopy and photoemission spectroscopy, are not applicable to the buried interfaces in general. A different approach to the interface problem is to study the cross section. By combination of high resolution transmission electron microscopy and electron energy-loss spectroscopy, the valence of the atoms at the interface has been identified with nanometer-scale resolution.[1,8,9] However, sample treatment by ion milling or mechanical polish may cause an artificial effect on the interface properties.

In contrast to the techniques mentioned above, optical second-harmonic generation (SHG) is a convenient probe to study buried interfaces.[10–13] In the electric-dipole (ED) approximation, the nonlinear polarization $\boldsymbol{P}$ as the source of SHG is given by

$$\boldsymbol{P}_i(2\omega) = \chi^{(2)}_{ijk}\boldsymbol{E}_j(\omega)\boldsymbol{E}_k(\omega), \tag{1}$$

where $\boldsymbol{E}(\omega)$ is the fundamental electric field with frequency ω and $\chi^{(2)}_{ijk}$ is the second-order susceptibility. Equation (1) indicates that SHG is forbidden in centrosymmetric materials.[10] It is allowed only at surfaces and interfaces that break the centrosymmetry. Since $\chi^{(2)}$ depends on the site symmetry, the SHG is drastically changed by subtle local modulations. Without modifying the sample, the buried interfaces are thus accessible by the SHG technique provided that it lies within the penetration depth of light ($\sim$100 nm). Magnetic SHG from the interfaces of perovskite manganite superstructures has been reported recently.[14,15]

In this paper, we report on nonlinear spectroscopic investigation and theoretical calculation of a manganite interface. The interface we study here is formed between $LaMnO_3$ (LMO) and $SrMnO_3$ (SMO). The nominal valences of the Mn ions of the respective manganites in the bulk are 3+ and 4+. They are insulators, but in solid solution, they exhibit a very complex phase diagram because of the aforementioned competition.[2] A natural question is whether the interfacial layer is equivalent to a bulk $La_{0.5}Sr_{0.5}MnO_3$ crystal or not. Because SHG is sensitive to the asymmetry of the crystal field of the Mn ion at the interface, we are able to single out the spectral feature reflecting the interfacial electronic state. By comparing with a Hartree-Fock calculation, we assigned it to an interface-bound charge transfer excitation, which is not expected from bulk LMO, SMO, and $La_{0.5}Sr_{0.5}MnO_3$. The calculation also suggests that there is no metallic $La_{0.5}Sr_{0.5}MnO_3$ at the interface.

Four distinct types of thin films were grown on $(LaAlO_3)_{0.3}$-$(SrAl_{0.5}Ta_{0.5}O_3)_{0.7}$ (LSAT) substrates by pulsed laser deposition: LMO/LSAT, SMO/LSAT, LMO/SMO/LSAT, and SMO/LMO/LSAT. Perovskite type LSAT(001) was chosen as the substrate because its lattice constant (3.87 Å) is close to the ones of bulk LMO (3.95 Å) and bulk SMO (3.81 Å) so that we can expect epitaxial growth. The substrate temperature was kept at 760 °C for

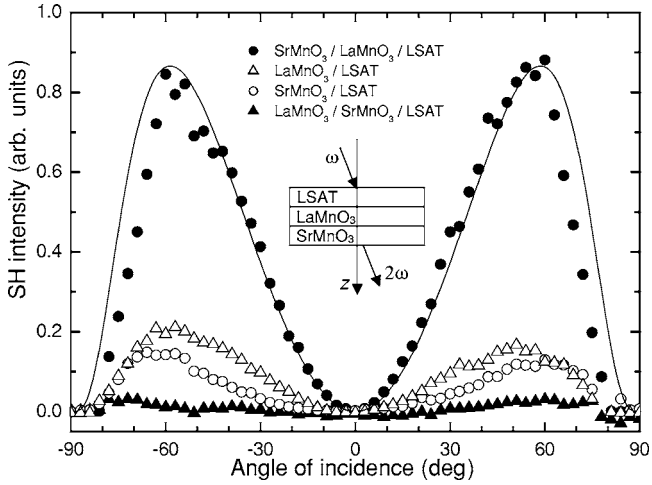

FIG. 1. Angular dependence of the SH intensities of manganite thin films at 2.74 eV as SH photon energy. The solid line is obtained from a model calculation based on the Maxwell equations for a heterostructure with an effective nonlinear medium localized at the interface. The angle of incidence is given with respect to the sample normal. The inset shows a schematic of the manganite heterostructure ($SrMnO_3/LaMnO_3/LSAT$).

LMO/SMO/LSAT and SMO/LMO/LSAT, 790 °C for SMO/LSAT, and 800 °C for LMO/LSAT, and the oxygen pressure was 0.1 mTorr during the deposition. The films were grown in the two-dimensional layer-by-layer mode, which is confirmed by the oscillation of the specular spot intensity in the reflection high-energy electron diffraction. The thickness of each layer was regulated to be 4–5 unit cells. Terraces with about 100 nm width and the step height of one unit cell were observed in atomic force microscopy images.[16]

The SHG measurements were performed at room temperature in air. An optical parametric amplifier with 150 fs light pulses pumped by an amplified Ti:sapphire laser system at 1 kHz repetition rate was used to produce the fundamental light. The fundamental photon energy ranged between 0.82 and 1.57 eV. The angle of incidence was varied from -90° to 90° by means of Maker fringe technique.[17] The fundamental light was *p* polarized and the SH light was detected as *p* polarized. The fundamental light is incident on the back of the substrate in order to avoid absorption of SH light in the yellow-colored LSAT substrate. Since the intensity and the width of the incident light pulses fluctuate shot by shot, the signal was normalized by SHG from urea powder. Typically 5000 pulses were averaged. The calibration of the manganite thin-film SH spectra was done relative to that of α-quartz. The Maker fringe of a *Y*-cut α-quartz slab with 1 mm thickness was measured and fitted by a model calculation.[18] The finite spectral width of the 150 fs incident light was taken into account for fitting the Maker fringe pattern of the α-quartz. For the $\chi^{(2)}$ dispersion of α-quartz, Miller's rule was applied.[19]

Figure 1 shows the angular dependence of the SH intensities of the four samples at an SH photon energy of 2.74 eV. The signal from the substrate alone was negligible. We confirmed the square dependence of the SH intensity on the input power in the range of 5–50 mJ/cm^2. On the basis of symmetry consideration of the input/output polarization, SHG from electric-quadrupole and magnetic-dipole was excluded. Other films twice and four times as thick did not show an increase of SH intensity. Therefore, bulk contributions are ignored as well. Thus, it is reasonable to consider that the ED-type SH source is located in almost one-unit cell layer. This is also confirmed by the theoretical calculation as discussed later. There are three types of interfaces; air-manganite, manganite-manganite, and manganite-substrate. The interfaces of air-LMO, air-SMO, LMO-SMO, SMO-LMO, LMO-LSAT, and SMO-LSAT are denoted as aL, aS, LS, SL, Lℓ, and Sℓ, respectively. The peak SH intensities for four samples ($I_{\mathrm{LMO/LSAT}}=0.20, I_{\mathrm{SMO/LSAT}}=0.15, I_{\mathrm{LMO/SMO/LSAT}}=0.02, I_{\mathrm{SMO/LMO/LSAT}}=0.86$) shown in Fig. 1 already indicate that SHG is sensitive to the crystal field asymmetry at the interface and the interference of SHG from different interfaces is important. Note that linear optical spectra cannot distinguish LMO/SMO/LSAT and SMO/LMO/LSAT samples.

The $\chi^{(2)}$s from interfaces all contribute coherently to SHG. By combining SMO/LSAT and LMO/LSAT films face to face, we found that χ^{aL} and χ^{aS} have the same sign and similar magnitude. Furthermore, the contribution from $\chi^{\mathrm{S}\ell}$ and $\chi^{\mathrm{L}\ell}$ is small. This conclusion is also confirmed by measuring the SHG of films grown on a different substrate ($LaSrAlO_4$). Thus the SH intensities from various films can be written in terms of $\chi^{(2)}$ as

$$I_{\mathrm{LMO/LSAT}} \propto |\chi^{\mathrm{aL}}|^2, \tag{2}$$

$$I_{\mathrm{SMO/LSAT}} \propto |\chi^{\mathrm{aS}}|^2, \tag{3}$$

$$I_{\mathrm{LMO/SMO/LSAT}} \propto |\chi^{\mathrm{aL}} + \chi^{\mathrm{LS}}|^2, \tag{4}$$

$$I_{\mathrm{SMO/LMO/LSAT}} \propto |\chi^{\mathrm{aS}} + \chi^{\mathrm{SL}}|^2. \tag{5}$$

The polarity of the SL interface in the sample leads to $\chi^{\mathrm{LS}}=-\chi^{\mathrm{SL}}$ in Eqs. (4) and (5). There are four equations [Eqs. (2)–(5)] for three variables. However, one set of $\chi^{(2)}$s can satisfy all the equations self-consistently, confirming our assertion that $\chi^{\mathrm{S}\ell}$ and $\chi^{\mathrm{L}\ell}$ are negligible.

The peak at around 60° in Fig. 1 is consistent with the assumed tetragonal symmetry (4*mm*). In this symmetry, the following $\chi^{(2)}$ tensors are allowed: $\chi^{(2)}_{xzx}=\chi^{(2)}_{yzy}=\chi^{(2)}_{xxz}=\chi^{(2)}_{yyz}$, $\chi^{(2)}_{zxx}=\chi^{(2)}_{zyy}$, and $\chi^{(2)}_{zzz}$, where *z* is normal to the interface. As shown in Fig. 1 we fit the angular dependence of the SH intensity to a model based on the Maxwell equations for a multilayer structure with an effective nonlinear medium with one unit cell thickness at the interface. Thus we estimate the $\chi^{(2)}$ value of SMO/LMO/LSAT as $\sim 10^{-6}$ esu. The $\chi^{(2)}$ value are corroborated by the theoretical calculation.

In order to investigate the contributing electronic processes, SH spectroscopy was performed in the range 1.64–3.14 eV. Figure 2 illustrates the calibrated SH intensity. The spectra is monotonously increasing as a function of photon energy, except for a resonance peak at around 2.0 eV in

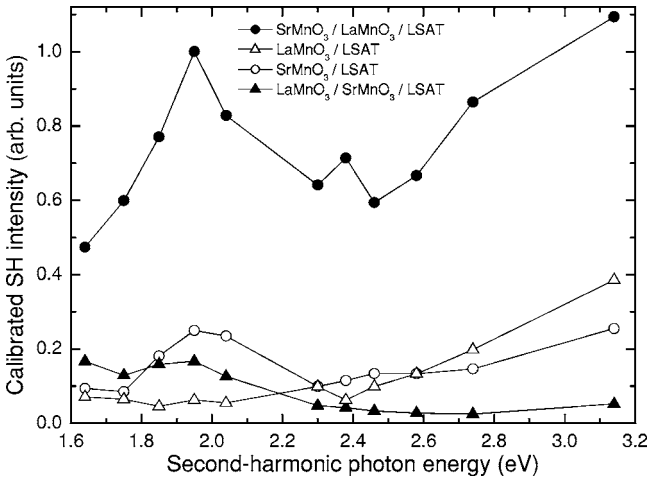

FIG. 2. Calibrated SH spectra of the manganite thin films as a function of SH photon energy. The spectra are normalized to the peak SH intensity of $SrMnO_3/LaMnO_3/LSAT$ at about 2 eV.

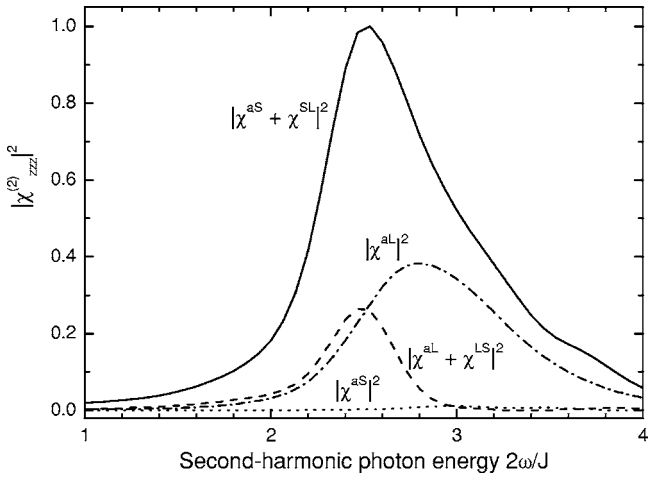

FIG. 3. The $|\chi^{(2)}_{zzz}|^2$ spectra based on the p-d model (see Ref. 24). The spectra are normalized so that the peak $|\chi^{aS}+\chi^{SL}|$ is unity, which corresponds to 1.184×10^{-6} esu.

SMO/LMO/LSAT, SMO/LSAT, and LMO/SMO/LSAT. The broad peak is not observed in the optical spectra of bulk LMO, SMO, and $La_{0.5}Sr_{0.5}MnO_3$.[20]

Now that the contributing $\chi^{(2)}$s are identified, we can compare the results with a theoretical calculation. The calculation was performed for a model, in which a number of layers are stacked along the z-axis in a sequence of $[MnO_2\text{-}LaO]_n\text{-}MnO_2\text{-}[SrO\text{-}MnO_2]_n$. We adopt a tight-binding p-d-type Hamiltonian, $\mathcal{H}=\mathcal{H}_d+\mathcal{H}_p+\mathcal{H}_{dp}$, where the Mn $3d$ and O $2p$ electrons are taken into account explicitly and the La and Sr ions are assumed to be point charges. The strongly interacting Mn e_g electrons which couple ferromagnetically with the localized t_{2g} spins are described by $\mathcal{H}_d$. The O $2p$ degree of freedom introduced in $\mathcal{H}_p$ and the electron hopping between the Mn e_g and O $2p$ orbitals in $\mathcal{H}_{dp}$ are essential for the SH spectra. The Jahn-Teller coupling between the e_g orbital and the lattice distortion is included in $\mathcal{H}_d$. Details of $\mathcal{H}$ for the bulk manganites are presented in Ref. 21.

The electronic structures are calculated by the Hartree-Fock (HF) method[21] where spin, charge, and orbital order parameters are introduced in each layer designated by m and the in-plane momentum $\vec{k}_\parallel$. Unrenormalized energy level $\varepsilon_d(m)[\varepsilon_p(m)]$ for $d(p)$ orbital is given in the ionic model where the Madelung potential[22] is obtained self-consistently with the calculated electron densities. The SHG spectra formulated in the HF scheme[23] is given as

$$\chi^{(2)}_{zzz}=-\frac{Ne^3}{\hbar^2}\sum_{m,n(\neq m),l,\vec{k}_\parallel} X_{mn}X_{nl}X_{lm}(F_1+F_2), \qquad (6)$$

and

$$F_1=\frac{f_{ml}}{\varepsilon^3_{lm}(2\varepsilon_{lm}-\varepsilon_{nm})(\omega-\varepsilon_{lm})}+\frac{f_{nl}}{\varepsilon^3_{nl}(2\varepsilon_{nl}-\varepsilon_{nm})(\omega-\varepsilon_{nl})},$$

$$F_2=\frac{16}{\varepsilon^3_{mn}(2\omega-\varepsilon_{mn})}\left\{\frac{f_{ml}}{\varepsilon_{nm}-2\varepsilon_{lm}}+\frac{f_{nl}}{\varepsilon_{nm}-2\varepsilon_{nl}}\right\}, \qquad (7)$$

with the difference of the Fermi distribution functions $f_{ij}=f_F(\varepsilon_i)-f_F(\varepsilon_j)$ and that of the HF energies $\varepsilon_{ij}=\varepsilon_i-\varepsilon_j$. Here, $X_{nm}(\equiv\langle n|X|m\rangle)$ is the matrix elements of the current operator

$$X=-t\sum_{i,\delta=\pm a\hat{z},\sigma}\delta\{d^\dagger_{3z^2-r^2\sigma}(i)p_{z\sigma}(i+\delta)-\text{H.c.}\}, \qquad (8)$$

with the transfer integral t and the Mn-O bond length a. The operator $d_{3z^2-r^2\sigma}(i)$ $[p_{z\sigma}(i)]$ is introduced for the $d_{3z^2-r^2}$ (p_z) electron with spin σ at site i. The film thickness is chosen to be $n=4$, reflecting the experimental condition. Larger n results in similar SH characteristics, which indicates the SHG comes only from the interface. Thus both the experiment and calculation capture the essential physics at the interface.

By restricting the summation of site i in Eq. (8), we can calculate the contributions to $\chi^{(2)}_{zzz}$ from different parts of the film separately. This is possible because the electronic states are sufficiently localized along the film normal. Note that the bulk LMO and SMO are insulators. As is verified experimentally, no contribution to $\chi^{(2)}_{zzz}$ is found from layers away from the interfaces and single MnO_2 layers at the interfaces carry most of the SH contribution. The calculated $|\chi^{(2)}_{zzz}|^2$s are shown in Fig. 3 in the form of SH intensities that correspond to the experiment [see Eqs. (2)–(5)]. The SH photon energy 2ω in the horizontal axis is normalized by the exchange coupling J at a Mn site being around 1 eV. Two features are worth noting; (i) χ^{SL}, χ^{aS}, and χ^{aL} have the same sign, and (ii) χ^{SL} is the largest among them. As a result, $I_{SMO/LMO/LSAT}$ determined by $|\chi^{aS}+\chi^{SL}|$ is the largest. These features are in good agreement with the experimental observations. The absolute value of $|\chi^{aS}+\chi^{SL}|$ at the peak in Fig. 3 is 1.184×10^{-6} esu. The calculated results also explain the experimentally observed $\chi^{(2)}$ value ($\sim10^{-6}$ esu) for the SMO/LMO/LSAT sample. In Fig. 3, negligible χ^{aS} means that interfacial χ^{SL} alone brings almost all $\chi^{(2)}$ value, which is about ten times as high as the highest $\chi^{(2)}$ component $(\chi^{(2)}_{xzx})$ of $BaTiO_3$ with the $4mm$ point group.[10] The large $\chi^{(2)}$ value in the manganite heterostructure mainly comes from the large electric field gradient of the static electric field at the interface which is particular to the strongly correlated

electron systems. It should be added, however, that the optical transition of the SHG process under consideration is close to resonance, which enhances the $\chi^{(2)}$ value.

The SH spectra are dominated by the two-photon absorption processes where the spectra enhance resonantly when 2ω is close to the charge-transfer excitation energies in Eq. (7). In bulk LMO and SMO, the charge-transfer excitations are $(e_g)^1(2p)^6 \rightarrow (e_g)^2(2p)^5$ and $(e_g)^0(2p)^6 \rightarrow (e_g)^1(2p)^5$, respectively. At the interface between LMO and SMO, a unique electronic state emerges, in which transitions from the O $2p$ state in LMO to the empty e_g state in SMO, and from the O $2p$ state in SMO to the upper Hubbard band in LMO are dominant. This leads to the enhancement of $2\omega/J \sim 2.5$, corresponding to the peak around 2.0 eV in Fig. 2.

However, the calculated results are not consistent with a peak at 2.0 eV in SMO/LSAT and no peak in LMO/LSAT in experiments. This may be due to the choice of the calculation parameter values which are determined by linear optical spectra reflecting 100 nm thick bulk properties of LMO and SMO.

The Mn valency of the interfacial layer sandwiched between LaO layer and SrO layer is 3.5+ but no metallicity shows up. This is in stark contrast to the case of Ti oxide[1] and demonstrates the extreme confinement of the two-dimensional electronic state in manganites. In fact, it has been known that, while the bulk $La_{0.6}Sr_{0.4}MnO_3$ is a metal in the ground state, $La_{0.6}Sr_{0.4}MnO_3$ in the form of 5 unit cell layers is insulating when separated by insulating layers thicker than 3 unit cells.[5]

In conclusion, we found an interface-bound charge transfer excitation between $LaMnO_3$ and $SrMnO_3$ by optical second-harmonic spectroscopy and a theoretical calculation. The interface second-order susceptibility $\chi^{(2)}$ is $\sim 10^{-6}$ esu, which is ten times higher than the highest $\chi^{(2)}$ component of $BaTiO_3$. The large nonlinearity mainly comes from the steep gradient of the static electric field at the interface. The calculation indicates no metallic $La_{0.5}Sr_{0.5}MnO_3$ phase at the interface, reflecting the strong electron correlations in manganites.

We are appreciative to M. Izumi for the use of his samples in the initial feasibility study. T.S. would like to thank M. Fiebig and B.B. Van Aken for valuable discussion. This work was supported by JSPS KAKENHI (15104006 and 16540305), MEXT TOKUTEI (16076207), NAREGI and CREST. Part of the numerical calculation has been performed by supercomputers in IMR, Tohoku University, and ISSP, University of Tokyo.

[1] A. Ohtomo, D. A. Muller, J. L. Grazul, and H. Y. Hwang, Nature (London) **419**, 378 (2002); S. Okamoto and A. J. Millis, *ibid.* **428**, 630 (2004).

[2] *Colossal Magnetoresistive Oxides*, edited by Y. Tokura (Gordon and Breach, London, 2000).

[3] Y. Okimoto, Y. Ogimoto, M. Matsubara, Y. Tomioka, T. Kageyama, T. Hasegawa, H. Koinuma, M. Kawasaki, and Y. Tokura, Appl. Phys. Lett. **80**, 1031 (2002).

[4] T. Satoh, Y. Kikuchi, K. Miyano, E. Pollert, J. Hejtmánek, and Z. Jirák, Phys. Rev. B **65**, 125103 (2002).

[5] M. Izumi, Y. Ogimoto, Y. Okimoto, T. Manako, P. Ahmet, K. Nakajima, T. Chikyow, M. Kawasaki, and Y. Tokura, Phys. Rev. B **64**, 064429 (2001).

[6] K. S. Takahashi, M. Kawasaki, and Y. Tokura, Appl. Phys. Lett. **79**, 1324 (2001).

[7] Y. Ogimoto, M. Izumi, A. Sawa, T. Manako, H. Sato, H. Akoh, M. Kawasaki, and Y. Tokura, Jpn. J. Appl. Phys., Part 2 **42**, L369 (2003).

[8] J. Verbeeck, O. I. Lebedev, G. Van Tendeloo, and B. Mercey, Phys. Rev. B **66**, 184426 (2002).

[9] F. Pailloux, D. Imhoff, T. Sikora, A. Barthélémy, J. -L. Maurice, J. -P. Contour, C. Colliex, and A. Fert, Phys. Rev. B **66**, 014417 (2002).

[10] Y. R. Shen, *The Principles of Nonlinear Optics* (Wiley, New York, 2002).

[11] T. F. Heinz, in *Nonlinear Surface Electromagnetic Phenomena*, edited by H. -E. Ponath and G. I. Stegeman (Elsevier, Amsterdam, 1991).

[12] E. Matthias and F. Träger eds., Appl. Phys. B: Lasers Opt. 68, (1999).

[13] A. Kirilyuk, J. Phys. D **35**, R189 (2002).

[14] Y. Ogawa, H. Yamada, T. Ogasawara, T. Arima, H. Okamoto, M. Kawasaki, and Y. Tokura, Phys. Rev. Lett. **90**, 217403 (2003).

[15] H. Yamada, Y. Ogawa, Y. Ishii, H. Sato, M. Kawasaki, H. Akoh, and Y. Tokura, Science **305**, 646 (2004).

[16] T. Satoh, Th. Lottermoser, M. Fiebig, Y. Ogimoto, H. Tamaru, M. Izumi, and K. Miyano, J. Appl. Phys. **97**, 10A914 (2005).

[17] P. D. Maker, R. W. Terhune, M. Nisenoff, and C. M. Savage, Phys. Rev. Lett. **8**, 21 (1962).

[18] N. Bloembergen and P. S. Pershan, Phys. Rev. **128**, 606 (1962).

[19] R. C. Miller, Appl. Phys. Lett. **5**, 17 (1964).

[20] J. H. Jung, K. H. Kim, T. W. Noh, E. J. Choi, and J. Yu, Phys. Rev. B **57**, R11043 (1998).

[21] R. Maezono, S. Ishihara, and N. Nagaosa, Phys. Rev. B **57**, R13993 (1998).

[22] D. E. Parry, Surf. Sci. **49**, 433 (1975); D. E. Parry, *ibid.* **54**, 195 (1976).

[23] E. Ghahramani, D. J. Moss, and J. E. Sipe, Phys. Rev. Lett. **64**, 2815 (1990); E. Ghahramani, D. J. Moss, and J. E. Sipe, Phys. Rev. B **43**, 8990 (1991).

[24] Parameter values used for the numerical calculation are the intra-orbital Coulomb interaction for the e_g electrons $U/J=6.75$, the superexchange interaction between the nearest-neighboring t_{2g} spins $J_{AF}/J=0.1$, the d–p transfer integral $t/J=0.8$, and the dielectric constant at infinite frequency $\varepsilon_\infty=2$. The exchange interaction at a Mn site J is around 1 eV. These values are chosen on the basis of the previous estimations and the linear-optical spectra in bulk manganites.